SYNTHESIS AND CHARACTERISATION OF SOD-, CAN- AND JBW-TYPE STRUCTURES BY HYDROTHERMAL REACTION OF KAOLINITE AT 200^{O}C

SINTESIS Y CARACTERIZACION DE ESTRUCTURAS TIPO SOD, CAN Y JBW POR REACCION HIDROTERMICA DE CAOLINITA A 200^{O}C

CARLOS RIOS REYES

Profesor Titular, Escuela de Geología, Universidad Industrial de Santander, Bucaramanga, Colombia, carios@uis.edu.co

CRAIG DENVER WILLIAMS

School of Applied Sciences, University of Wolverhampton,England, c.williams@wlv.ac.uk

CLIVE ROBERTS

School of Applied Sciences, University of Wolverhamptont, Wolverhampton WV1 1SB, England, c.l.roberts@wlv.ac.uk

Received for review July 24 th, 2009, accepted April 22th, 2010, final version May, 15 th, 2010

ABSTRACT: Low-silica zeolitic materials like SOD, CAN and JBW crystallized after hydrothermal transformation of kaolinite in the system Na_2O–Al_2O_3–SiO_2–H_2O at 200ºC, with or without the addition of a structure-directing agent. The synthesis products were characterized by XRD, SEM, FTIR, ^{29}Si and ^{27}Al MAS-NMR and TGA. After dissolution of kaolinite in alkaline medium, co-crystallization of SOD and CAN, likely via a metastable LTA intermediate, was followed by a transformation to JBW-type structure.

KEYWORDS: Low-silica zeolitic materials, hydrothermal, synthesis, kaolinite, dissolution

RESUMEN: Materiales zeolíticos bajos en sílice como SOD, CAN y JBW cristalizaron después de la reacción hidrotérmica de caolinita en el sistema Na_2O–Al_2O_3–SiO_2–H_2O a 200ºC, con o sin adición de un agente director de estructura. Los productos de la síntesis fueron caracterizados por DRX, MEB, espectroscopía FTIR, ^{29}Si- y ^{27}Al-RMN y TGA. Después de la disolución de la caolinita en medio alcalino, co-cristalizaron SOD y CAN, probablemente a partir de una fase intermedia metastable (LTA), lo cual fue seguido por una transformación a la estructura tipo JBW.

PALABRAS CLAVE: Materiales zeolíticos bajos en sílice como, hidrotérmica, síntesis, caolinita, disolución

1. INTRODUCTION

Zeolites are crystalline aluminosilicates of the alkaline or alkaline earth metals with three-dimensional frameworks composed of $[SiO_4]^{4-}$ and $[AlO_4]^{5-}$ tetrahedral that corner-share to form different open structures. The zeolite structures only contain (-Si-O-Al-) linkages when the Al:Si ratio is exactly 1.0 and the Loewenstein rule is obeyed. They form uniform pores in the nanometer range and enclose regular internal channels and cavities of discrete sizes and shapes.

Low-silica zeolites (LSZs) with Al/Si ratio of 1:1 like zeolite A (LTA), sodalite (SOD), zeolite P (GIS), zeolite X (FAU) and Nepheline Hydrate I (JBW) are relatively rare [1]. These zeolites exhibit the highest ion exchange capacity and have important industrial applications. They are used as adsorbents or substitute for conventional phosphatic builder, viz. sodium tripolyphosphate (STP), which is well known to cause eutrophiction. However, their preparation from chemical sources of silica and alumina is expensive and, therefore, their use in environmental remediation is restricted due to prohibitive costs, which can be overcome by seeking low-cost raw materials like kaolinite for inexpensive zeolite synthesis. The conversion of kaolinite to metakaolinite by heating above the dehydroxylation temperature activates the clay [2-3] and the reactivity of metakaolinite varies with the thermal treatment [4], affecting the zeolitization process as discussed by several authors [5-11]. Kaolinite can be used for LSZs synthesis because SiO_2 and Al_2O_3 contents are similar to each other.

The alkaline hydrothermal transformation of kaolinite and metakaolinite to zeolites is well known, with

zeolite LTA as the most common synthesis product [3]. Zeolite X is another important product, which can be prepared from kaolinite usually with additional silica sources [12-13]. Low-silica X (LSX) zeolite is much more difficult to prepare, requiring careful control during the synthesis conditions [7, 9, 14-15]. Sodalite (SOD) and zeolite P (GIS) can be prepared as well [6, 9]. Buhl et al. [16-17] synthesized nitrate cancrinite (CAN) from kaolin under hydrothermal conditions at 80ºC. Some zeolites with higher Si/Al ratio, such as mordenite, ZSM-5, and NaY have been prepared by using kaolin and additional silica sources as starting materials [18]. The LSZs synthesis has been widely researched at temperatures less than 100ºC. However, there are few studies on zeolite synthesis from kaolin under higher temperatures. Hackbarth et al. [19] prepared carbonate cancrinite from kaolin in NaOH medium at the temperature of 200ºC, while a disordered intermediate phase between the CAN and SOD structure was obtained at the lower reaction temperature of 80ºC. However, according to Coombs et al. [20], CAN and SOD are feldspathoids with a three-dimensional aluminosilicate host framework. They have structural similarities, since their aluminosilicate layers of six-membered rings are identical to each other, and the structures only differ in the stacking sequences of these layers [21]. CAN $[Na_8Al_6Si_6O_{24}(NO_3)_2]$ has a hexagonal framework which contains small ε-cages made of six-membered rings and large channels consisting of 12-membered rings, which can incorporate cations such as Na^+, K^+ and Ca^{2+}, as well as inorganic anions such as CO_3^{2-}, OH^- and NO_3^- and water molecules [22-24]. According to Zhao et al. [25], the 12-membered channel in CAN might be easier to access than the ε-cage. SOD, $[Na_8Al_6Si_6O_{24}(NO_3)]$, has a cubic framework contains only β-cages (or "sodalite" cages) made up of 6-membered rings, and each cage contains water molecules or cation/anion pairs [24]. The shape of β-cages is a truncated octahedron. In general, these materials, as most zeolites, display fully open structures with pores directly connected by large channels separated by relatively thin aluminosilicate walls and small molecules [1, 26]. On the other hand, zeolite JBW is unusual, taking into account that a zeolitic portion of the structure is separated from the next by a layer of the cristobalite structure containing non-hydrated cations [27].

Healey and co-workers [1, 28] synthesized pure aluminosilicate JBW after hydrothermal treatment of kaolin in a mixture solution of NaOH and KOH at 225ºC and Na/Rb–AlGe–JBW from a mixture of sodium and rubidium-containing reagent at 225ºC. Shimizu and Hamada [29] synthesized large crystals with a JBW framework and other zeolites from a ceramic tube as an aluminosilicate source by a bulk material dissolution technique. Tripathia and Parise [30] prepared aluminogermanate analogues of JBW (Na–AlGe–JBW) in the reactant containing tetramethyl ammonium hydroxide (TMAOH) at 140ºC. Lin et al. [31] investigated the hydrothermal synthesis of zeolite SOD, CAN and JBW with metakaolinite as the raw material at 200ºC. Preliminary experimental work by Ríos [44] reveals the formation of a JBW-type structure from metakaolinite using precipitated SiO_2. Ríos et al. [32] synthesized several kaolinite-based zeotypes, including a nearly pure JBW-type structure using NaOH solutions and triethylamine (TEA) as a structure-directing agent (SDA) at 200ºC. Wei et al. [33] reported for the first time the synthesis of JBW-type zeolites with aerosil and aluminium triisopropoxide as starting materials in a sodium hydroxide medium, in which phenol was used as an organic solvent. The JBW-type structure is one of the lesser-studied zeolites, which was first reported by Barrer and White [34]. According to Healey et al. [1], a subsequent work referred to this zeotype inappropriately as Nepheline Hydrate I and its crystal structure was solved partially in 1982 by Hansen and Fälth [35]. The JBW-type structure is unusual because one part of its structure is separated from the next by what is effectively a layer of the cristabolite structure containing non hydrated cations [35]. According to Weller [26], the existence of this semi-condensed block helps to stabilizes higher aluminium contents and the JBW structure is invariably found for an Al/Si ratio of 1:1. The structure was found to be orthorhombic with cell parameters a = 16.426(1)Å, b = 15.014(5)Å and c = 5.224(5)Å, crystallizing in the Pna21 space group [1]. According to Weller [26], the JBW-type structure represents a true hybrid-layered oxide/zeolite structure with alternating channels and condensed non-hydrated oxide blocks. This material obviously has structural relationships with pillared clays [36] and the layered complex metal oxides of the type $CsNbTi_2O_7$ [37].

In this work, we investigate the hydrothermal transformation of kaolinite into a JBW-type structure at 200ºC. We also investigate the effect of the use of TEA as an SDA for zeolite synthesis, taking into account that many types of high-silica zeolites (HSZs) can be synthesized under hydrothermal conditions using

excess water and employing quaternary ammonium salts, amines or other organic substances as an SDA.

2. EXPERIMENTAL PROCEDURE

2.1 Materials

The starting material used in this work was a well crystallized, fine grained kaolinite (≤ 2 μm) from St. Austell (UK), which is distributed under the name Supreme Powder, supplied by English China Clay. Other reagents used in the activation of kaolinite were: sodium hydroxide, NaOH, as pellets (99%, Aldrich Chemical Company, Inc.); TEA (triethanolamine - 99%, BDH Laboratory Supplies) and distilled water using standard purification methods.

2.2 Kaolinite-based synthesis of low-silica zeolites (KSLSZs)

Zeolite synthesis was carried out by hydrothermal conversion of kaolinite (silica and alumina source) in alkaline medium. A calculated amount of alkali hydroxide pellets was added to distilled water in reaction plastic beakers (150-250 ml) to prepare 1.33M and 3.99M NaOH solutions; kaolinite was then mixed with the alkaline solutions to produce a reaction gel with a specific molar composition. To evaluate the influence of SDA, we carried out hydrothermal treatments with an alkaline medium with the addition of a calculated amount of SDA to explore the opportunity of obtaining different zeolitic products. The progressive addition of reagents was carried out under stirring conditions until they dissolved to homogenize the reaction gels. The crystallization was carried out by hydrothermal synthesis under static conditions in PTFE vessels (Cowie Technology Ltd) of 65 ml at 100°C and 20 ml stainless steel autoclaves at 200°C for different reaction times. Once the activation time was reached, the reactors were removed from the oven and quenched in cold water to stop the reaction. After hydrothermal treatment, the reaction mixtures were filtered and washed with distilled water to remove excess alkali until the pH of the filtrate became neutral. Then, the samples were oven dried at 80°C overnight. Hydrogel pH was measured before and after hydrothermal treatment. The dried samples were weighted and kept in plastic bags for characterization. Table 1 presents the experimental conditions used for zeolite synthesis.

Table 1. Synthesis conditions for transformation of kaolinite into SOD-, CAN- and JBW-type structures

Test No.	Molar composition of the reaction gel	Hydrothermal reaction T (°C)	t (h)	As-synthesized zeolitic products
1	$3Na_2O:Al_2O_3:2SiO_2:88.3H_2O$	100	6	LTA, SOD, CAN
2	$3Na_2O:Al_2O_3:2SiO_2:88.3H_2O$	100	72	LTA, SOD, CAN
3	$3Na_2O:Al_2O_3:2SiO_2:88.3H_2O$	100	120	LTA, SOD, CAN
4	$3Na_2O:Al_2O_3:2SiO_2:88.3H_2O$	200	24	SOD, CAN, JBW
5	$3Na_2O:Al_2O_3:2SiO_2:88.3H_2O$	200	96	SOD, CAN, JBW
6	$3Na_2O:Al_2O_3:2SiO_2:88.3H_2O$	200	168	SOD, CAN, JBW
10	$Na_2O:Al_2O_3:2SiO_2:0.5TEA:86.3H_2O$	200	6	SOD, CAN
11	$Na_2O:Al_2O_3:2SiO_2:0.5TEA:86.3H_2O$	200	24	SOD, CAN
12	$Na_2O:Al_2O_3:2SiO_2:0.5TEA:86.3H_2O$	200	48	SOD, CAN, JBW
13	$3Na_2O:Al_2O_3:2SiO_2:0.5TEA:88.3H_2O$	200	6	SOD, CAN
14	$3Na_2O:Al_2O_3:2SiO_2:0.5TEA:88.3H_2O$	200	24	SOD, CAN, JBW
15	$3Na_2O:Al_2O_3:2SiO_2:0.5TEA:88.3H_2O$	200	48	SOD, CAN, JBW

LTA, zeolite LTA; SOD, sodalite; CAN, cancrinite; JBW, JBW-type zeolite

2.3 Characterization of the raw material and synthesis products

The chemical composition of the raw material was investigated by XRF in a Shimazu EDX 800 HS XRF spectrometer. The quantification of the elements was carried out using the method of fundamental parameters (FP) with the software DXP-700E Version 1.00 Rel. 014. X-ray diffraction (XRD) on untreated kaolinite and synthesis products was performed with a Philips PW1710 diffractometer operating in Bragg-Brentano geometry using secondary graphite monochromated Cu-Kα radiation (40 kV and 40 mA). Data collection was carried out in the 2θ range 3-50°, with a step size of 0.02°, a divergent slit of 1.0º, and a dwell time of 2 s. Crystalline phases were identified using the ICDD-JCPDS powder diffraction database. The relative intensity yields were obtained from normalized XRD intensities of the major reflection for each material. The morphology of the synthesis products was examined by scanning electron microscopy (SEM) in a ZEISS EVO50 scanning electron microscope and the chemical composition of mineral phases was studied using the EDXS mode, under the following analytical conditions: I probe 1 nA, EHT = 20.00 kV, beam current 100 μA, Signal A = SE1, WD = 8.0 mm. Fourier transform infrared (FT-IR) spectroscopy was carried out by using a Mattson Genesis II FT-IR spectrometer in the 4000-400 cm^{-1} region. However, we discuss only the 1200-400 cm^{-1} region, because it is where the spectra showed remarkable changes. Solid-state magic angle spinning nuclear magnetic resonance (MAS-NMR) spectra for ^{29}Si and ^{27}Al, respectively, were collected at room temperature on a Varian Unity INOVA spectrometer under the following analytical conditions: MAS probe 7.5 and 4.0 mm; frequency 59.6 and 78.1 MHz; spectral width 29,996.3 and 100,000.0 Hz; acquisition time 30 and 10 μs; recycle time 120 and 0.5 s; number of repetitions 15 and 2200; spinning rate 5040 and 14,000 Hz; pulse angle (DP) 90.0 and 18.9°. The chemical shifts were referenced to tetramethylsilane (TMS) for ^{29}Si and 1 M $AlCl_3$ aqueous solution for ^{27}Al.

Thermogravimetric analyses were performed on a Mettler Toledo TG 50 thermobalance. Samples ~ 15-20 mg were heated under nitrogen gas flow (20 ml/min) between 25-700ºC at a rate of 20ºC/min.

3. RESULTS AND DISCUSSION

3.1 Raw material

Kaolinite, $Al_2SiO_5(OH)_4$, is a mineral species with a specific composition (SiO_2 = 46.55%; Al_2O_3 = 39.50%; H_2O = 13.96%). The material used in this research is a kaolinite-rich product with some impurities such as illite, muscovite, and halloysite identified by XRD (Figure 1).

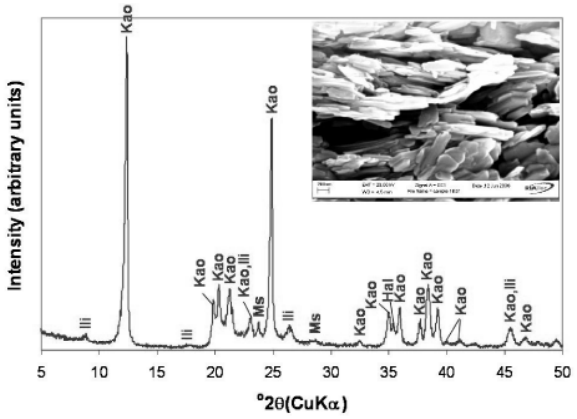

Figure 1. X-ray diffraction pattern of the kaolinite-rich raw material and its SEM image. Kao, Kaolinite; Ili, illite; Ms, muscovite; Hal, halloysite

Kaolinite can be recognized by its platy morphology and hexagonal outlines, with small, well-formed hexagonal plates loosely packed, defining an orientation. Rocks that are rich in kaolinite are known as china clays or kaolin. The chemical composition of kaolinite was 46.44% SiO_2, 38.80% Al_2O_3, TiO_2 0.03%, Fe_2O_3 0.52%, MgO <0.08%, Na_2O <0.33%, K_2O 0.69 and LOI 15.35%, with a SiO_2/Al_2O_3 = 1.2.

3.2 Synthesis products

3.2.1 XRD analysis

The XRD patterns of unreacted and reacted kaolinite treated with 3.99M NaOH solutions for various reaction periods are presented in Figure 2. The hydrothermal treatment of kaolinite under these experimental conditions resulted in the co-crystallization of SOD and CAN, along with metastable LTA. According to Ríos [38], a higher NaOH concentration in the synthesis solution leads to faster dissolution of the original kaolinite, accompanied by more crystalline zeolitic materials, as shown by an increase of the relative intensity of the XRD peaks of SOD and CAN.

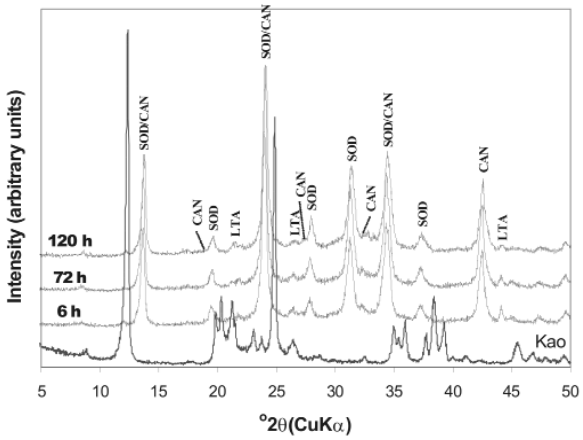

Figure 2. X-ray diffraction patterns of synthesis products after reaction of kaolinite at 100ºC for several times (tests 1-3, Table 1)

The activation of kaolinite at a higher temperature promoted the co-crystallization of the JBW-type structure of high intensity peaks with traces of SOD and CAN (Figure 3). Lin et al. [31] concluded that the reaction at higher temperature is advantageous for the synthesis of JBW. No interesting changes were observed using TEA at low temperature (results not shown). However, the use of SDA at high temperature (Figures 4 and 5) reveals clear evidence of a phase transformation SOD+CAN → JBW, as shown by the co-crystallization of SOD and CAN at shorter reaction times (6 h), followed by the formation of the JBW, as a main crystalline phase, at longer reaction times (24-48 h). However, the final synthesis products are composed by a mixture of SOD, CAN, and JBW, similar to what is observed in Figure 3.

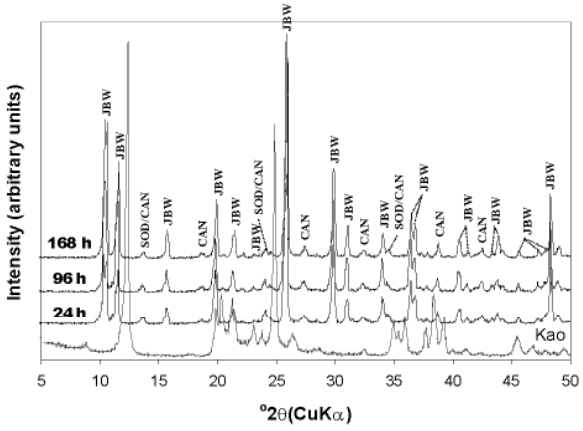

Figure 3. X-ray diffraction patterns of synthesis products after reaction of kaolinite at 200ºC for several times (tests 4-6, Table 1)

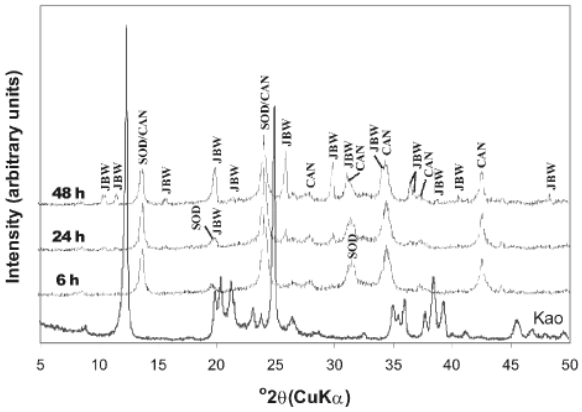

Figure 4. X-ray diffraction patterns of synthesis products after reaction of kaolinite at 200ºC for several times, using TEA as an SDA (tests 7-9, Table 1)

In general, at high temperature, the raw kaolinite was quickly dissolved; the crystallinity of the kaolinite-based feldspathoids showed a constant behaviour, except using a high NaOH concentration and adding TEA, which promoted a decrease in the crystallinity of SOD and CAN at longer reaction times. On the other hand, the crystallinity grade of the JBW-type structure increased using a high NaOH concentration and longer reaction times.

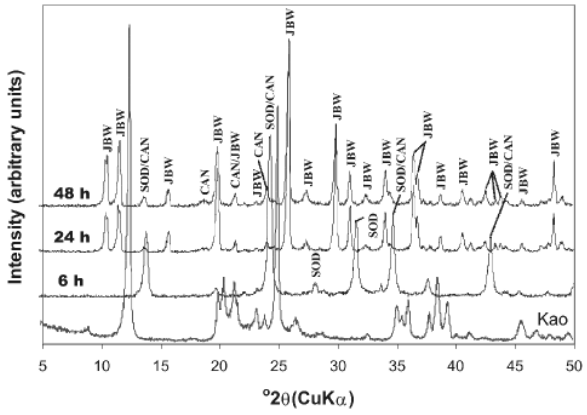

Figure 5. X-ray diffraction patterns of synthesis products after reaction of kaolinite at 200ºC for several times, using TEA as a SDA (tests 10-12, Table 1)

3.2.2 SEM analysis

SEM images (Figure 6) illustrate the occurrence of the as-synthesized zeolitic products obtained after activation of kaolinite, revealing a change in morphology of the original surface of the platy particles of kaolinite.

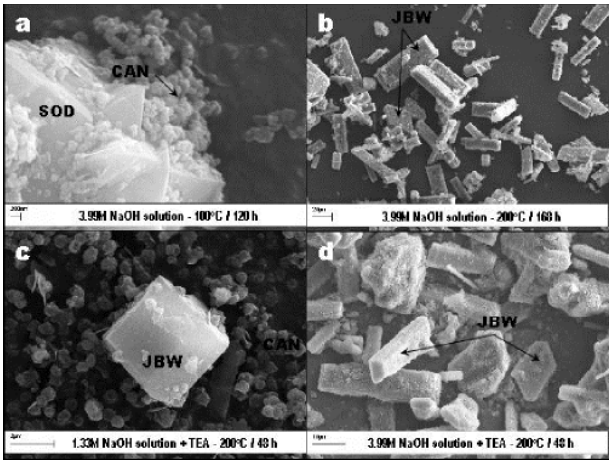

Figure 6. SEM images showing several synthesis products obtained by hydrothermal treatment of kaolinite in the presence of NaOH

A transformation of SOD into CAN is illustrated in Figure 6a. SOD shows a wedge-shaped blade morphology whereas CAN occurs as lepispheres composed of intergrown thin disks. The phase transformation SOD → CAN has been reported elsewhere [37-40]. These morphological features are consistent with the mixture of LTA, SOD and CAN observed in the XRD patterns. Characteristic long prismatic lath-like crystals of JBW, with pseudohexagonal cross sections, are illustrated in Figure 6b. Similar morphologies were observed by Wei et al. [33] in JBW-type zeolite obtained by phenol solvothermal synthesis. A JBW crystal with a tubular morphology associated to lepispheric aggregates of CAN is observed in Figure 6c. Healey et al. [28] reported similar tubular morphologies in aluminogermanate possessing the zeolite JBW framework topology. Prismatic lath-like and tubular crystals of JBW, with pseudohexagonal cross sections, are illustrated in Figure 6d.

3.2.3 FT-IR analysis

The FT-IR spectra of the original kaolinite and as-synthesized products obtained after its hydrothermal treatment with alkaline solutions are shown in Figure 7.

The characteristic OH-stretching vibrations at 3687 cm^{-1} (surface OH stretching) and 3619 cm^{-1} (inner OH stretching), as well as the bands at 1116, 1031, 1008, 938 (surface OH bending), 913 (inner OH bending), 797, 790, and 754 cm^{-1}, in kaolinite disappeared with reaction time. In general, the characteristic bands of kaolinite shift of transmittance to lower wavenumbers

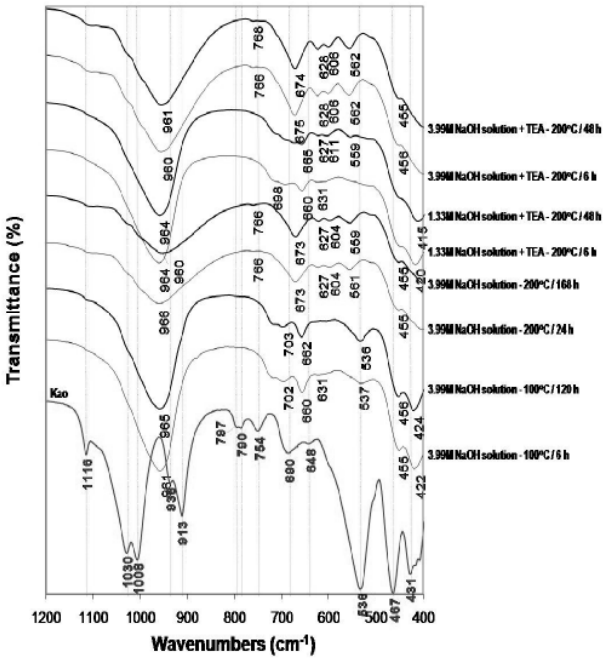

Figure 7. FTIR spectra of unreacted and reacted kaolinite with NaOH solutions

indicates that there are more Al substitution in tetrahedral sites of the silica framework with NaOH acting as a structure modifier as reported in other studies [41-43].

The absorption bands of the synthesis products at low temperature show the asymmetric and symmetric vibration bands characteristic of a mixture of LTA zeolite, SOD, and CAN in the region 1200-400 cm^{-1}. Barnes et al. [38] summarized the reported assignments of vibrations for SOD and CAN in this range. Coincident with the disappearance of kaolinite, characteristic zeolite bands appeared on the spectra, including the asymmetric Al-O stretch located in the region of 1250-950 cm^{-1}, and their symmetric Al-O stretch located in the region of 770-660 cm^{-1}. The region 1200-850 cm^{-1} shows a single vibration band centred at 960-965 cm^{-1}, associated with the presence of CAN. The transmittance of the asymmetric stretch of the Si-O-Al in the SOD framework consists of a single band at 980 cm^{-1}, which split into four bands at 1110, 1050, 1020, and 960 cm^{-1} assigned to CAN [38]. However, this study reports only the bands at 975 and 960-965 cm^{-1}, corresponding to SOD and CAN, respectively. The region 850-750 cm^{-1} reveals a weak vibration band at 766-768 cm^{-1}, characteristic of CAN. Several bands in the region 750-650 cm^{-1} indicate the presence of a mixture of SOD and CAN in the as-synthesized products

The bands in the region 650-500 cm^{-1} are related to the presence of the double rings (D4R and D6R) in the framework structures of the zeolitic materials [2]. In this region, three characteristic vibration bands are reported for the first time, which can be attributed to the presence of six-rings of the dehydrated region and eight-rings of the hydrated section of the JBW zeolite. The bands in the region 500-420 cm^{-1} are related to internal tetrahedron vibrations of Si-O and Al-O of the synthetic zeolites. The region 800-400 cm^{-1} can be considered as the 'fingerprint' region not only for LTA zeolite, SOD, and CAN as suggested in previous studies [38, 42] but also for JBW zeolite.

3.2.4 ^{29}Si and ^{27}Al MAS-NMR

The structural unit of kaolinite consists of a Si-O tetrahedral sheet and an Al-O(OH) octahedral sheet. Figure 8 shows the ^{29}Si and ^{27}Al MAS-NMR spectra of the raw kaolinite and as-synthesized JBW.

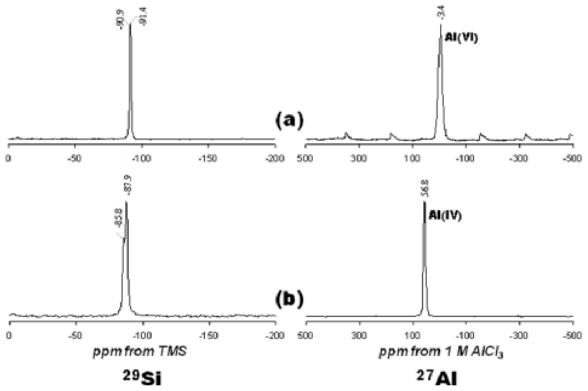

Figure 8. ^{29}Si and ^{27}Al NMR spectra of the (a) raw kaolinite and (b) JBW-type structure (treated kaolinite in 3.99 M NaOH solutions – 200 °C / 166 h)

The ^{29}Si MAS-NMR spectrum of kaolinite (Figure 8a) shows two signals at -90.9 and -91.4 ppm attributed to the existence of two different but equally populated silicon sites. Two resonance peaks at -85.8 and -87.9 ppm (Figure 8b) were observed for JBW. Similar results have been reported by Healey et al. [1] and Lin et al. [31] to confirm the characteristic framework of the JBW-type structure. They attributed the smaller of the two peaks (at 85.8 ppm) to Si(1), whereas other two chemically similar silicon atoms, Si(2) and Si(3), lead to the larger of the two peaks (at 87.9 ppm). The ^{27}Al MAS-NMR spectrum of the unreacted kaolinite (Figure 8a) consists of a single resonance at -3.4 ppm and is largely octahedral Al. A single resonance at 56.8 ppm (Figure 8b) can be assigned to tetrahedral Al in the framework of JBW. The transformation

of kaolinite into JBW resulted in a shift of Al from octahedral to tetrahedral coordination, which is likely due to the dissolution of kaolinite and the subsequent precipitation of a JBW-type structure. The amount of Al(6) is greatest in kaolinite where the initial Al concentration was larger compared with that in the synthesis product. The decrease in the Al(6)/Al(4) ratio can be explained by the dissolution of kaolinite, with Al coordination changing from octahedral to tetrahedral, which is consistent with the formation of JBW.

3.2.5 TG analysis

DTG curves of KSLSZs are shown in Figure 9. The as-synthesized products show up to four dehydration steps. The position of these DTG peaks and the number of dehydration steps can be attributed to the different compensating cation-water binding energies as well as to the different energy associated with the diffusion of the desorbed water through the porous structure of the as-synthesized products; their weight loss percentages reflects the water loss from the zeolite structure, and the amount of desorbed water is related with the number of compensation cations in the framework of the zeolite (Covarrubias et al., 2006).

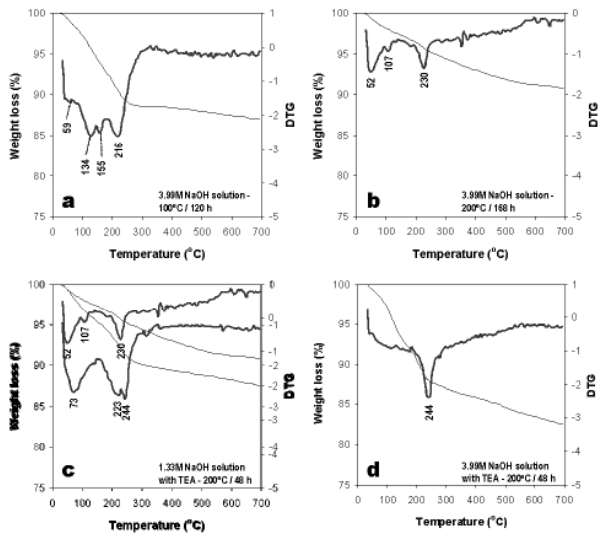

Figure 9. DTG curves from 25 to 700 °C of the synthesis products obtained from the kaolinite-rich raw material; (a), (b), (c) and (d) refer to tests 3, 6, 9 and 12, respectively, in Table 1

The peaks observed between 46 and 59 °C correspond to surface water in zeolitic materials; the peaks observed between 107 and 155 °C indicate zeolitic water, although in some cases in this range of temperature up to two peaks occur, which can be explained by the heterogeneous nature of the as-synthesized products. There are also some peaks in the range of temperature 216-244 °C. The peaks at 223 and 244 °C are related to the vaporizing of TEA. However, sometimes these peaks are broad, which indicate that water and TEA are coming out from the zeolite. The as-synthesized zeolitic products obtained after hydrothermal transformation of kaolinite in solutions of 3.99M NaOH at 100 °C for 120 h display the highest weight loss (13.02%), which indicates that these products have a higher amount of water. The lowest weight loss (8.10%) was obtained for zeolitic materials formed after the reaction of kaolinite in solutions of 3.99M NaOH + TEA at 200 °C for 48 h.

3.3 Crystallization of JBW-type zeolite

Table 1 lists the compositions in the reacting mixture in the autoclave for zeolite synthesis. In the absence of SDA in the gel, the crystallization of zeolites showed different synthesis products, according to the temperature of reaction. A mixture of LTA zeolite, SOD, and CAN was obtained at 100 °C, as demonstrated by XRD patterns shown in Figure 2. On the other hand, SOD, CAN, and JBW crystallized at 200 °C (Figure 3). These results indicate that TEA is not necessary for crystallization of JBW-type zeolite from TEA-free hydrogels. The formation of these zeolitic materials is in agreement with the previous study by Ríos et al. [32], which suggest that SOD- and CAN-type structures are the main zeolitic phases at shorter reaction times (6 h), whereas JBW was formed from hydrogels at longer reaction times (24-48 h). To research the effect of using SDAs, the hydrothermal synthesis using TEA was conducted (Figures 4 and 5). These results were supported by the fact that the Na_2O/Al_2O_3 ratio controlled the degree of crystallinity of the JBW-type structure and TEA worked as an SDA on the crystallization of this zeolite in the hydrothermal synthesis method. Lin et al. [31] studied the influence of the molar ratios of Na_2O/Al_2O_3 and H_2O/Na_2O in the reactant on the crystallization of JBW-type structures, with LTA and JBW zeolites at lower and higher Na_2O/Al_2O_3 ratios, respectively. According to these authors, by increasing the ratio of Na_2O/Al_2O_3 (1.45-1.94), JBW zeolite crystallizes. On the other hand, in the reactant system with the same ratio of Na_2O/Al_2O_3, the crystallinity of the zeolite decreased by increasing the ratio of H_2O/Na_2O from 14.4 to 21.3. However, our results indicate that this zeolite can form using molar ratios of Na_2O/Al_2O_3 and H_2O/Na_2O of 1-3 and 29.4-86.3, respectively. As described

above, TEA is not essential for the crystallization of the JBW-type structure using this method in the system Na_2O-SiO_2-Al_2O_3-H_2O, with no crystallization of JBW zeolite at shorter reaction times, which is in agreement with results obtained by Ríos [44], who tested several SDAs during the transformation of kaolinite by hydrothermal treatment in alkaline solutions under different experimental conditions without any interesting differences in zeolitic phases and crystallinity. To optimize the synthesis process when adding organic templates to the chemical system does not mean that their effect as structure-directing and pore-filling agents would be successful and therefore this should be sufficiently demonstrated. The hydrogels with a lower Na_2O/Al_2O_3 ratio yielded JBW zeolite more slowly than those with a higher Na_2O/Al_2O_3 ratio, as demonstrated by XRD patterns shown in Figures 4 and 5, respectively. Authors consider that SDAs have not shown any important effect on this system. Therefore, it is assumed that the concentration of the alkaline activating solution would control the first appearance of JBW zeolite and its crystallinity.

4. CONCLUSIONS

KSLSZs such as SOD, CAN, and JBW were successfully synthesized from kaolinite in the **system Na_2O–Al_2O_3–SiO_2–H_2O** at 200°C**,** with or without the addition of TEA as an SDA. There were two major chemical processes involved in the reaction between kaolinite and the alkaline medium: the dissolution of kaolinite followed by the formation of zeolitic materials. SDAs play an important role in the crystallization of zeolitic materials. A sequence of transformation SOD → CAN → JBW is

proposed in this study. Although the use of anionic surfactants (which are SDAs) for the synthesis of zeolites was strongly desired, results demonstrate that the preparation of zeolites from the kaolinite-rich product used in this study using an anionic surfactant such as TEA was unsuccessful, taking into account that TEA was not encapsulated in the pore channels of the as-synthesized JBW zeolite. Therefore, it seems that this SDA has a negligible or even slightly negative effect on JBW zeolite formation.

ACKNOWLEDGMENTS

We thank the Programme Alban, the European Union Programme of High Level Scholarships for Latin America, scholarship No. E05D060429CO, and the Universidad Industrial de Santander for funding C.A. Ríos. Special thanks to School of Applied Sciences at University of Wolverhampton for allowing us the use of the research facilities. We thank Dr Townrow and Mrs Hodson for assistance in collecting XRD and SEM data, respectively, and Dr Apperley and the EPSRC solid state NMR Service, University of Durham, for MAS NMR spectra. Finally, we are thankful to Prof. Mark T. Weller from the University of Southampton for his useful comments and suggestions.

REFERENCES

[1] HEALEY, A.M., JOHNSON, G.M., WELLER, M.T. The synthesis and characterisation of JBW-type zeolites. Part A: Sodium/potassium aluminosilicate, $Na_2K[Al_3Si_3O_{12}]\cdot 0.5H_2O$. Microporous and Mesoporous Mater. 37, 153–163, 2000.

[2] BRECK, D.W. Zeolite Molecular Sieves: Structure, Chemistry and Use, 1st Ed., John Wiley, New York, 1974.

[3] HELLER-KALLAI, L., LAPIDES, I. Reactions of kaolinites and metakaolinites with NaOH - Comparison of different samples (Part 1). Appl. Clay Sci. 35, 99-107, 2007.

[4] ROCHA, J., KLINOWSKI, J. ^{29}Si and ^{27}Al magic-angle-spinning NMR studies of the thermal transformation of kaolinite. J. Phys. Chem. Miner. 17, 179-186, 1990.

[5] LUSSIER, R. A novel clay-based catalytic material-preparation and properties. J. Catal. 129, 225-237, 1991.

[6] MURAT, M., AMOKRANE, A., BASTIDE, J.P., MONTANARO, L. Synthesis of zeolites from thermally activated kaolinite. Some observations on nucleation and growth. Clay Miner. 27, 119–130, 1992.

[7] AKOLEKAR, D., CHAFFEE, A., HOWE, R.F. The transformation of kaolin to low-silica X zeolite. Zeolites 19, 359-365, 1997.

[8] PERISSINOTTO, M., LENARDA, M., STORARO, L., GANZERLA, R.J. Solid acid catalysts from clays: Acid leached metakaolin as isopropanol dehydration and 1-butene isomerization catalyst. J. Mol. Catal. A 121, 103-109, 1997.

[9] CHANDRASEKHAR, S., PRAMADA, P.N. Investigation on the synthesis of zeolite NaX from Kerala kaolin. J. Porous Mater. 6, 283-297, 1999.

[10] DEMORTIER, A., GOBELTZ, N., LELIEUR, J.P., DUHAYON, C. Infrared evidence for the formation of an intermediate compound during the synthesis of zeolite Na–A from metakaolin. Int. J. Inorg. Mater. 1, 129-134, 1999

[11] Xu, M., Cheng, M., Bao, X., Liu, X., Tang, D. Growth of zeolite KSO1 on calcined kaolin microspheres. J. Mater. Chem. 9, 2965-2966, 1999.

[12] De Lucas, A. Uguina, M.A., Covian, I., Rodriguez, L. Synthesis of 13X zeolite from calcined kaolins and sodium silicate for use in detergents. Ind. Eng. Chem. Res. 31, 2134-2140, 1992.

[13] De Lucas, A. Uguina, M.A., Covian, I., Rodriguez, L. Use of Spanish natural clays as additional silica source to synthesize 13X zeolite from kaolin. Ind. Eng. Chem. Res. 32, 1645-1660, 1993.

[14] Basaldella, E.I., Tara, J.C. Synthesis of LSX zeolite in the Na/K system. Influence of the Na/K ratio, Zeolites 11, 243-248, 1995.

[15] Basaldella, E.I., Kikot, A., Tara, J.C. Effect of pellet pore size and synthesis conditions in the in situ synthesis of LSX zeolite. Ind. Eng. Chem. Res. 34, 2990-2996, 1995.

[16] Buhl, J.C., Taake, C., Stief, F., Fechtelkord, M. The crystallisation kinetics of nitrate cancrinite Na7.6 [AlSiO4]6(NO3)1.6 (H2O)2 under low temperature hydrothermal conditions. React. Kinet. Catal. Lett. 69, 15 - 21, 2000.

[17] Buhl, J.C., Stief, F., Fechtelkord, M., Gesing, T.M., Taphorn, U., Taake, C. Synthesis, X-ray diffraction and MAS NMR characteristics of nitrate cancrinite Na7.6[AlSiO4]6(NO3)1.6(H2O)2. J. Alloys Compd. 305, 93-102, 2000.

[18] Im, K.C., Takasaki, Y., Endo, A. Hydrothermal Synthesis of Zeolites in NaOH Solution from Hadong Kaolin of Korea: In Case of Starting Materials of Kaolin with Addition of Silica. Nippon Kagaku Kaishi, 348-354, 1997.

[19] Hackbarth, K., Fechtelkord M., Buhl, J.C. The crystallization kinetics of Na7.4[AlSiO4]6(CO3)0.7 ×4H2O: An intermediate Phase between cancrinite and sodalite, grown under low temperature hydrothermal conditions. React. Kinet. Catal. Lett. 65, 33-39, 1998.

[20] Coombs, D.S., Alberti, A., Armbruster, T., Artioli, G., Colella, C., Galli, E. Recommended nomenclature for zeolite minerals: Report of the subcommittee on zeolites for the International Mineralogical Association, Commission on New Minerals and Mineral Names. Can. Mineral. 35, 1571-1606, 1997.

[21] Okubo,T., Wakihara, T., Plévert, J., Nair, S., Tsapatsis, M., Ogawa, Y., Komiyama, H., Yoshimura, M., Davis, M.E. Heteroepitaxial Growth of a Zeolite. Angew. Chem. Int. Ed. 40, 1069-1071, 2001.

[22] Barrer, R.M. Zeolites and Clay Minerals as Sorbents and Molecular Sieves. Academic Press, London, 1978.

[23] HUND, F. Nitrate-, thiosulfate-, sulfate- and sulfide cancrinite. Z. Anorg. Allg. Chem. 509, 153-160, 1984.

[24] Gerson, A.R., Zheng, K. Bayer process plant scale: transformation of sodalite to cancrinite. J. Cryst. Growth 171, 209-218, 1997.

[25] Zhao, H., Deng, Y., Harsh, J.B., Flury, M., Boyle, J.S. Alteration of Kaolinite to Cancrinite and Sodalite by Simulated Hanford Tank Waste and its impact on Cesium retention. Clays Clay Miner. 52, 1-13, 2004.

[26] WELLER, M.T. Where zeolites and oxides merge: semi-condensed tetrahedral frameworks. J. Chem. Soc., Dalton Trans., 4227-4240, DOI: 10.1039/b003800h, 2000.

[27] FEREY, G. The new microporous compounds and their design. C. R. Acad. Sci., Ser. Ii Fascicule C, Chimie 1, 1-13, 1998.

[28] Healey, A.M., Henry, P.F., Johnson, G.M., Weller, M.T., Webster, T.M., Genge, A.J. The synthesis and characterisation of JBW-type zeolites. Part B: Sodium/ rubidium aluminogermanate, Na2Rb[Al3Ge3O12]·H2O. Microporous and Mesoporous Mater. 37, 165-174, 2000.

[29] Shimizu, S., Hamada, H. Synthesis of giant zeolite crystals by a bulk material dissolution technique. Micropor. Mesopor. Mater. 48, 39-46, 2001.

[30] Tripathi, A., Parise, J.B. Hydrothermal synthesis and structural characterization of the aluminogermanate analogues of JBW, montesommaite, analcime and paracelsian. Micropor. Mesopor. Mater. 52, 65-78, 2002.

[31] Lin, D.-Ch., Xu, X.-W., Zuo, F. Zuo, Long, Y.-C. Crystallization of JBW, CAN, SOD and ABW type zeolite from transformation of metakaolin. Microporous and Mesoporous Mater. 70, 63-70, 2004.

[32] Ríos, C.A., Williams, C.D., Maple, M.J. Synthesis of zeolites and zeotypes by hydrothermal transformation of kaolinite and metakaolinite. Bistua 5, 15-26, 2007.

[33] Wei, B., Wang, Y., Xin, M.-H., Qiu, S.-L. Phenol solvothermal synthesis of JBW-type zeolites. Chem. Res. Chin. Univ. 23, 511-513, 2007.

[34] Barrer, R.M., White,. E.A.D. The hydrothermal chemistry of silicates. Part II. Synthetic crystalline sodium aluminosilicates. J. Chem.. Soc., 1561-1571, 1952.

[35] Hansen, S., Fälth, L. X-ray study of the nepheline hydrate I structure. Zeolites 2, 162-166, 1982.

[36] Gil, A., Vicente, M.A., Gandia, L.M. Main factors controlling the texture of zirconia and alumina pillared clays Micropor. Mesopor. Mater. 34, 115-125, 2000.

[37] Hervieu, M., Raveau, B. A layer structure: The titanoniobate CsTi2NbO7. J. Solid State Chem. 32, 161-165, 1980.

[38] Ríos, C.A., Williams, C.D., Fullen, M.A. Nucleation and growth history of zeolite LTA synthesized from kaolinite by two different methods. Appl. Clay Sci. 42, 446-454, 2009.

[37] Barnes, M.C., Addai-Mensah, J., Gerson, A.R. The mechanism of the sodalite-to-cancrinite phase transformation in synthetic spent Bayer liquor. Microporous Mesoporous Mater. 31, 287-302, 1999.

[38] Barnes, M.C., Addai-Mensah, J., Gerson, A.R. A methodology for quantifying sodalite and cancrinite phase mixtures and the kinetics of the sodalite to cancrinite phase transformation. Microporous Mesoporous Mater. 31, 303-319, 1999.

[39] Barnes, M.C., Addai-Mensah, J., Gerson, A.R. The solubility of sodalite and cancrinite in synthetic spent Bayer liquor. Colloids Surf., A 157, 106-116, 1999.

[40] Choi, S., Crosson, G., Mueller, K.T., Seraphin, S., Chorover, J. Clay mineral weathering and contaminant dynamics in a caustic aqueous system. II. Mineral transformation and microscale partitioning. Geochim. Cosmochim. Acta 69, 4437-4451, 2005.

[41] Aronne, A., Esposito S., Pernice, P. FT-IR and DTA study of lanthanum aluminosilicates glasses. Mater. Chem. Phys. 51, 163–168, 1997.

[42] Aronne, A., Esposito, S. Ferone, C., Pansini, M., Pernice, P. FT-IR study of the thermal transformation of barium-exchanged zeolite A to celsian. J. Mater. Chem. 12, 3039–3045, 2002.

[43] Park, M., Choi, C.L., Lim, W.T., Kim, M.C., Choi, J., Heo, N.H. Molten-salt method for the synthesis of zeolitic materials: I. Zeolite formation in alkaline molten-salt system. Microporous and Mesoporous Mater. 37, 81-89, 2000.

[44] Ríos, C.A. Synthesis of zeolites from geological materials and industrial wastes for potential application in environmental problems [PhD Thesis]. Wolverhampton, West Midlands: University of Wolverhampton, 2008.